Energy, Mines and Resources Canada | Énergie, Mines et Ressources Canada

CANMET

Canada Centre for Mineral and Energy Technology | Centre canadien de la technologie des minéraux et de l'énergie

DEGRADATION OF SLAGLINE CHROME-MAGNESIA BRICKS IN SECONDARY STEELMAKING: FINAL REPORT

K.E. Bell and D.H.H. Quon
Ceramic Section
Mineral Processing Laboratory

June 1984

Project: MRP - 3.6.0.0.72
Electrodes and refractories for steelmaking

This document is an unedited interim report prepared primarily for discussion and internal reporting purposes. It does not represent a final expression of the opinion of the Canada Centre for Mineral and Energy Technology (CANMET)

Ce document est un rapport provisoire non-révisé et rédigé principalement pour fin de discussion et de documentation interne; il ne représente nullement l'expression définitive de l'opinion du Centre canadien de la technologie des minéraux et de l'énergie (CANMET)

MINERALS RESEARCH PROGRAM
MINERAL SCIENCES LABORATORIES
DIVISION REPORT MRP/MSL 84-76(IR)

MICROMEDIA
SEP 1 6 1984

DEGRADATION OF SLAGLINE CHROME-MAGNESIA BRICKS IN SECONDARY STEELMAKING: FINAL REPORT

by

K.E. Bell** and D.H.H. Quon*

ABSTRACT

This work was conducted in an attempt to gain a better understanding of the degradation of rebonded fused-grain chrome magnesia refractories used in secondary steelmaking under vacuum. This is considered a serious problem by the steel industry, and a need for its solution has been identified by the Canadian Iron and Steel Research Association.

The previously reported mechanism of slag corrosion of basic refractories has been confirmed by using scanning electron microscopy and energy dispersive X-ray techniques. The results showed that during contact of the slag with the refractories, the principal constituents such as CaO and SiO_2 were introduced into the bricks where they reacted to form silicates containing CaO-MgO-MnO solid solutions at the grain boundaries of chrome-spinel and periclase. Strength reduction of the refractory brick can also be due to other causes such as inhomgeneity of distribution of periclase and chrome-spinel crystals.

Both texture and elemental distribution of Si and Ca found in post-mortem studies of commercially slagged bricks have been reproduced in laboratory cup-test experiments. The development of cracks, and formation of silicates in the bricks due to slag penetration have been observed in the cup tests.

Another factor, the volatilization loss of MgO in vacuum at high temperature has been confirmed. It is suggested that, due to the loss of MgO, the bonding of the grains in the refractories is reduced.

**Head, Ceramic Section and *Research scientist, Mineral Processing Laboratory, Mineral Sciences Laboratories, CANMET, Energy, Mines and Resources Canada, Ottawa.

DÉGRADATION DES BRIQUES DE CHROME-MAGNÉSIE DU CORDON EN SIDÉRURGIE SECONDAIRE: RAPPORT FINAL

K.E. Bell** et D.H.H. Quon*

RÉSUMÉ

Les travaux ont eu pour but de mieux comprendre la dégradation des réfractaires de chrome-magnésie à grains fondus reliés utilisés sous vide en sidérurgie secondaire. Les sidérurgistes estiment que cette dégradation est un problème grave et la Canadian Iron and Steel Research Association pense qu'il doit être résolu.

Le mécanisme déjà signalé de la corrosion des réfractaires par la scorie a été confirmé par des études faisant appel à la microscopie électronique à balayage ainsi qu'à la radiographie à dispersion d'énergie. Ces études ont montré que pendant le contact de la scorie et des réfractaires, les principaux constituants de la première tel le CaO et le SiO_2 ont pénétré les réfractaires et réagi pour former des silicates contenant des solutions solides de CaO-MgO-MnO à la frontière des grains du chrome-spinel et du periclase. La réduction de la résistance des réfractaires peut aussi être attribuable à d'autres causes comme l'hétérogéinité de la distribution du periclase et des cristaux de chrome-spinel.

La texture et la distribution des éléments Si et Ca caractérisant des réfractaires scorifiés du commerce après leur usage ont été reproduites en laboratoire dans des essais en vase. Ont été observées pendant ces essais en vase. Ont été observées pendant ces essais la formation de fissures et la formation de silicates dans les réfractaires par suite de la pénétration de la scorie.

La présence d'un autre factuer, la perte par volatilisation sous vide à haute température du MgO, a été confirmée. Les résultats obtenus donnent à penser que la perte du MgO explique l'affaiblissement de la liaison des grains des réfractaires.

**Chef, Section de la céramique, et *chercheur, Laboratoire de traitement des minéraux, Laboratoires des sciences minérales, CANMET, Énergie, Mines et Ressources Canada, Ottawa.

CONTENTS

ABSTRACT i
RÉSUMÉ ii
INTRODUCTION 1
EXPERIMENTAL PROCEDURES 2
Materials 2
Microscopy 2
Cup Tests 2
Vapourization Loss 3
Thermal Shock Resistance 3
RESULTS AND DISCUSSION 4
EDXR Analysis of Used Brick 4
Laboratory Cup Tests 5
Thermal Shock Resistance 7
Vapourization Loss of Oxides into Vacuum 8
CONCLUSIONS 10
ACKNOWLEDGEMENTS 13
REFERENCES 13

TABLES

1. Compositions of the slags used for laboratory cup tests 14
2. Luminescent phases in the slag component and their approximate compositions 15
3. Test conditions for vapourization studies 16

FIGURES

1. SEM micrograph of typical slag-penetrated zone of a used brick, with EDXR maps of the major slag components Ca, Si and Mn 17
2. SEM micrograph of a fresh slag-brick contact zone, with EDXR maps showing the distribution of elements of interest 18
3. SEM micrographs of luminescent phases in slagged brick; Top: green octahedra with orange reaction rims; Bottom: white acicular crystals 19

4. SEM micrographs of luminescent phases in slagged brick; Top: green octahedron with reddish core; Bottom: green octahedron with orange rim in a field of blue dendrites 19
5. Optical micrograph showing slag penetration into wall of cup, x 125 20
6. Optical micrograph showing slag penetration into cup wall, x 250 20
7. Thin section of slag-penetrated cup showing silicates (white) in pores and along grain boundaries; transmitted light, crossed polars, x 50 21
8. Enlarged section of Fig. 7 showing silicate crystal habit; acicular and dendritic growths, x 250 21
9. Polished section of slag-penetrated cup, x 125 22
10. Thin section of slag-penetrated cup, transmitted light, crossed polars, x 50 22
11. Cross-sectioned cups after two cycles at 1700°C for 3 hours 22
12. Optical micrograph of fully slagged cup, showing similarity to microstructure of used brick, x 250 23
13. Thin section of fully slagged cup, showing interstitial silicates (white), transmitted light, crossed polars, x 125 23
14. SEM micrograph of fully slagged cup, with EDXR maps of distribution of elements of interest 24
15. SEM micrograph of fully slagged and bloated cup, with EDXR maps of elemental distribution of principal slag constituents 25
16. Linear thermal expansion of (A) unused brick, (B) slag-penetrated zone of used brick, and (C) unslagged (cold) end of used brick 26
17. Furnace vapour pressure profiles during oxide vapourization: (A) rfg Cr-Mg brick, overtemperature, (B) rfg Cr-Mg test cup, 1750°C, (C) rfg Cr-Mg brick, 1750°C, (D) periclase brick, 1650°C 27
18. Optical micrograph of vapourized surface (1750°C for 3 hours) 27
19. SEM micrograph showing exsolved spinel phase outlining the ghost grains of periclase (1650°C for 3 hours) 28
20. SEM micrograph of fracture surface perpendicular to Fig. 19 28
21. Fracture surface of unslagged (cold) end of used rfg Cr-Mg brick 29
22. Fracture surface of unused rfg Cr-Mg brick 29

INTRODUCTION

The degradation of the rebonded fused-grain chrome-magnesia (rfg Cr-Mg)refractory bricks used in the slagline of vessels for secondary steelmaking by the Vacuum Oxygen Decarburization (VOD) process has been examined using optical and scanning electron microscopy (SEM) and X-ray diffraction analysis (XRD) (1). Preliminary results indicated that the wide range of texture and nonuniform distribution of chrome-spinel and periclase in the chrome-magnesia bricks may have a bearing on the degradation of the refractory material during service. The mechanism of slag corrosion of these basic refractories has been ascribed to interaction of CaO and SiO_2 from the slag with the refractories to form calcium-magnesium silicates at the grain boundaries. The formation of these silicates, coupled with the likely presence of iron, probably decreased the refractoriness of the chrome-magnesia brick, forming liquid at much lower temperatures than anticipated. The presence of liquid phase silicates in the grain boundaries and the resulting structural weakness would render the bricks more susceptible to erosion under the strong agitation prevailing during oxygen blowing and argon stirring. At lower temperatures (between heats) the presence of another phase in the grain boundaries could also contribute to reduced resistance to thermal shock and increased spalling.

Another factor that may also contribute to the degradation of the refractories is the volatilization loss of oxides such as MgO and Cr_2O_3 in vacuum at high temperature. The loss of oxide constituents is accompanied by an increase in porosity and weakening of the intergranular bonds, thus exposing the refractories to increased slag penetration.

Based on the preliminary results summarized above, work was conducted in examining used and unused rebonded fused-grain chrome-magnesia bricks using the energy dispersive X-ray (EDXR) technique in an attempt to gain better resolution of the phases involved.

Further attempts were also made to examine the cause of cracks developed as a result of contact between slag and refractories. Volatilization of oxides into vacuum at high temperature, related to weakening of the intergranular bonds, was examined in some detail, as was the effect of both slag penetration and oxide vapourization on the potential for thermal spalling of the bricks in service.

This investigation forms part of a project to study the behaviour of refractories in VOD/VAD secondary steel-making vessels, identified as a serious problem by the Canadian Steel and Iron Research Association.

EXPERIMENTAL PROCEDURES

Materials

The materials used for this study were slag-attacked and unused rebonded fused-grain chrome-magnesia bricks, supplied by Atlas Steels Company, as used in the slagline of VOD-VAD vessels at the company's Welland, Ontario plant. The company also provided appropriate slag samples for reaction studies; the compositions of the slags and the calculated CaO/SiO_2 ratios are given in Table 1.

Microscopy

Both optical and scanning electron microscopy were employed for characterizing the degradation of bricks resulting from either contact with slag or due to volatilization loss of oxides at high temperature in vacuum. In addition, the energy dispersive X-ray technique (EDXR) was used to map the elemental distribution in the reaction products resulting from the interaction of the slag and brick.

Cup Tests

The stability of the refractories vs. slags was determined by the cup-test method, described in detail previously (1). In essence, small cups were prepared from unused bricks by cutting and core drilling. The hole was packed with ground slag, the cup was contained in a molybdenum safety crucible and heated under vacuum in a graphite resistance furnace to temperatures in the range from 1550 to 1750°C for periods of 1 to 3 h. Two different furnaces were used at various times and circumstances: the smaller*, holding a single cup, reached the predetermined temperature in approximately one hour; the larger**, with a capacity for up to 6 cups, required approximately 3 hours.

---

* Astro Industries Inc., California, U.S.A., Model 1000-2560

** GSC Vacuum Industries, Massachusetts, U.S.A., Model 91-840

Cooling was conducted under vacuum at the normal cooling rate of the respective furnaces. In addition, several experiments were conducted by repeated filling of the refractory crucible and reheating under the same conditions to allow for more extensive reaction between slag and brick.

Vapourization Loss

In the studies of the vapourization loss of oxides (MgO and/or Cr_2O_3) small cubes of unused chrome-magnesia brick were cut to about 1.4 x 1.4 x 0.6 cm with one face polished and used for the experimental work.

During the heating of the vacuum furnace, the temperature of the furnace was monitoring by using a Leeds and Northrup optical pyrometer, and vapour pressure changes in the vacuum chamber were continuously monitored by the vacuum gauge. The weight loss of the refractory brick due to volatilization of oxides was obtained by weighing the sample prior to and after heat treatment.

Thermal Shock Resistance

Specimens measuring approximately 50 x 50 x 100 mm were cut from used and unused brick: the specimens of used brick comprised about half slag-penetrated and half cold-end zones, proportioned along the long axis. Single specimens of each material were inserted, on end, in a preheated box furnace for ~15 min, then air-quenched for ~15 min. To ensure equal cooling so far as possible, the hot specimens were set on a suspended aluminum plate. The cool specimens were examined visually for cracks. When cracking occurred, the heat/quench cycle was repeated at the same or increased temperature to expand the cracks to failure and to examine the effect of cycling on the uncracked specimens.

The results from the thermal shock tests indicated the possibility that thermal spalling might be abetted by additional stresses arising from differential thermal expansion of the slag-penetrated zone and the unpenetrated cold end. Test specimens measuring 6 x 6 x 50 cm long were cut from an unused brick and from the slag-penetrated and cold zones of a used brick for determination of thermal expansion. Thermal expansions were measured dynamically from room temperature to 1000°C using a vertical-tube dilatometer with fused quartz extension media and an Ames dial. The rate of heating was 10°C/min and measurements were made to the nearest 0.0025 mm (0.005%). No allowance was made for the equivalent expansion of the fused quartz, considered negligible in this context.

RESULTS AND DISCUSSION

EDXR Analysis of Used Brick

A typical section from the slag-penetrated zone of a used brick was selected for examination by EDXR in conjunction with the scanning electron microscope. Area scans (maps) were obtained showing the distribution of the individual elements of interest (Fig. 1). Although essentially qualitative, the elemental distribution maps serve well to locate the phases previously identified by X-ray diffraction.

In this well-slagged section the fused grain has clearly recrystallized as chrome-magnesia spinel with a well-defined (111) morphology, with the interstices filled with lathlike recrystallized calcium-magnesium silicates previously identified (1) as complex mixtures of monticellite, forsterite/fayalite and akermanite or melilite. The small circular white spots in the micrograph are metal droplets that were entrained in the slag: the manganese, presumably also sourced in the metal, is widely distributed but appears to have preferentially been taken up in the spinel.

The brick/slag contact is shown in the micrograph of Fig. 2, along with EDXR maps of elemental distributions. This specimen is of some interest because it probably marks the onset of slag corrosion of a freshly spalled brick face. Even at this high magnification, there is a sharp demarcation between the slag and the apparently unreacted brick. The latter shows the typical structure of rebonded fused-grain material: periclase grains liberally sprinkled throughout with blebs of exsolved chrome spinel, with sparsely scattered subhedral crystals of chrome spinel. No crystallization is discernable in the slag although its microcrystalline nature has been previously shown by XRD and transmission microscopy. However, the EDXR maps show that the slag (Ca, Si and Al) has penetrated the grain boundaries to depths of over 200 μm (upper right corner). At the same time the protective chrome spinel rimming the fused grains has begun to dissolve, leading to concentrations of chrome and lesser amounts of magnesia in the adjacent slag.

The slag itself is very complex in nature: under electron bombardment some of the phases proved to be strongly luminescent, as shown in Fig. 3 and 4. The phases distinguished by their luminescent colours were analyzed by microprobe and their approximate compositions are given in Table 2, from which it can be deduced that the cooled slag consists primarily of solid solutions

of Ca-Mg-Mn silicates (which would be expected). Manganese appears to be present in minor or trace amounts and there is no indication that it plays a significant role in corrosion of the refractories, where it appears to substitute for chromium in the spinel structure.

By contrast, EDXR scans of an unused brick showed only chromium and magnesium, with only a trace of calcium and no silicon, confirming that the materials penetrating the grain boundaries of used bricks originated in the slag.

Laboratory Cup-Tests

In attempt to duplicate slag corrosion in the laboratory, a series of cup-tests were conducted at high temperatures in vacuum. Several tests were conducted to confirm the results previously obtained: slags 1, 3 and 5 (from the ladle after teeming) were heated at 1550°C for three hours, slags 2, 4 and 6 (taken on conclusion of the V.O.D. phase) at 1650°C for 3 hours. To ensure comparability, each set of cups was fired simultaneously in a large vacuum furnace.

In the tests at 1550°C, residues of slag remained in the cups after heating, indicating that penetration had been incomplete. Analysis of the residues by XRD indicated the phases beta dicalcium silicate, olivine and a trace of chrome spinel. Obviously some periclase had dissolved from the cup to form olivine and spinel. Similarly, optical microscopic examination of polished sections from the cups showed some form of slag penetration to depths of 100 to 250 μm (Fig. 5 and 6). A significant increase in porosity was noted, attributed to dissolution of the chrome-magnesia in the presence of insufficient slag to fill the resulting porosity. These cups showed none of the lenticular internal cracks noted previously in the slag-penetrated zones of test cups and in several of the used refractories. Their absence lends credence to the proposition that such cracks form along planes of microstructural non-uniformity (weakness) as a result of the blockage of pores by slag, which prevents the release of gases formed during dissolution and vapourization of brick components. It is evident from the figures that the periclase is highly susceptible to slag attack and is the first to dissolve, whereas the chrome spinel is more resistant, resulting in a structure comprised of ghost fused grains delineated by the exsolution blebs along with euhedral to anhedral spinel no longer bonded by interstitial periclase. In

thin section under crossed polars, silicates can be seen as interstitial materials (Fig. 7), occasionally in the typical lath-like morphology (Fig. 8).

At 1650°C, slags 2, 4 and 6 penetrated more completely; up to 500 μm into the walls of the cups, with little or no residue. The microstructures are in most respects identical to those at the lower temperature. Typical polished and thin sections are shown in Fig. 9 and 10 respectively.

Although these results tend to confirm earlier conclusions as to the mechanics of corrosion, the obvious disparities between laboratory and commercial conditions led to modification of the test conditions. To accelerate the rate of attack the test temperature was raised to 1700°C for 3 hours. To ensure an adequate supply of slag to fill the pores the cups were cycled twice, repacked with slag between heats. This had the added advantage of duplicating in part the recycling to which the ladles are subject. Under these conditions the depth of slag penetration increased, illustrated in Fig. 11. In addition, these cups developed the lenticular cracks previously noted and hypothesized to result from concentration of slag along zones of weakness, sealing the pores and trapping gases internally; as the surrounding mass is pyroplastic owning to the liquid phase along the grain boundaries, swelling occurs. In polished section, the typical microstructure of the slagged cups (Fig. 12) shows many of the characteristics of the used bricks. The sample contains euhedral chrome spinel and anhedral periclase bearing exsolution blebs of chrome spinel, in a matrix of lath-shaped crystals of silicates. The latter are clearly shown in the thin section under crossed polars of Fig. 13.

An SEM micrograph of a typical section of a thoroughly slag-penetrated cup is shown in Fig. 14, along with EDXR maps of the elements of principal interest. Remnantal components of the original cups are easily distinguished: well-rounded (partially dissolved) fused grains of periclase bearing exsolved blebs of spinel, and octahedral chrome spinel grains carrying reaction rims (light grey) of apparent different stoichiometry, either the result of interdiffusion of material from the slag (e.g., substitution for chrome of alumina or manganese dioxide) or, more probably, partial dissolution of the original chrome spinel followed by epitaxial crystal growth with material of modified composition from the melt. The interstices are filled with calcium silicates from the slag, including some white prismatic crystals not specifically identified but similar to those of Fig. 4 (Ca/Mg silicates). The magnesia remains concentrated in the partly dissolved periclase and can also

be seen in the lath-like white crystals. The iron, assumed to originate largely from the chrome ore and previously shown to concentrate in the periclase during the fusion process, follows the magnesia dissolved in the slag. Titanium (not illustrated) was a minor constituent distributed quite uniformly over-all, with some concentration in the larger white acicular crystals.

Further direct evidence of the mechanics of slag attack is shown in Fig. 15, where slag penetration (evidenced by the calcium and silicon EDXR maps) can be seen along not only the obvious structural weaknesses such as the elongated pore in the upper right and a similar weakness that has given rise to the formation of one of the previously noted bloated cracks, but also along the tightly bound grain boundaries of the mass in the centre of the photomicrographs.

Thermal Shock Resistance

A limited number of specimens of unused and half-slagged brick were examined for thermal shock resistance by cyclic insertion into a preheated furnace (air atmosphere) and air-quenching. Typically, tests were conducted between room temperature and 1000°C for 6 cycles. The half-slagged briquette developed a first incipient crack on the first quench cycle, the unused briquette developed a vestigial primary crack on the third cycle. However, whereas the primary crack in the half-slagged specimen continued to expand and grow with each cycle and an incipient secondary crack developed, the crack in the unused brick showed little change through 6 cycles. The furnace temperature was then raised to 1050°C and quenching continued for a further 6 cycles. At this point, the half-slagged specimen separated easily under finger pressure along the initial primary and secondary cracks and was observed to have developed a second set of incipient primary and secondary cracks in the lower (unslagged) half. The specimen of unused brick, on the other hand, was broken only with difficulty along the primary crack and could not be separated by hand along an incipient secondary crack that first developed after 2 cycles at the higher temperature. These results led to the conclusion that the unused brick could withstand thermal shock of on the order of 50°C greater than the used brick.

This cracking pattern is typical for specimens of this geometry, stressed by uniform heating and cooling from all 6 sides: primary failure occurs on a plane midway along the longer axis parallel to the ends, secondary failures along planes perpendicular to the primary cracks midway between the

sides (effectively quartering the end segments). The unused brick closely followed this pattern, although the fracture surface was rough as a result of the intergranular mode of failure. The plane of the primary fracture of the half-slagged specimen, however, was not geometrically regular but followed the surface of slag penetration; the fracture surface was smoother, showing both intergranular fracture and transverse fracture through several small thoroughly slag-penetrated zones.

This failure mode of the half-slagged brick suggests a possible concentration of stresses along the surface of slag penetration such as might be expected if the slag altered the coefficient of thermal expansion of the slagged zone, hence thermal expansions were measured of the unused brick, the slagged zone of a used brick and of the unslagged (cold) end of a used brick. The results are shown in Fig. 16. The differences between expansions of the unslagged and slagged materials are minor and are not considered significant relative to the previously identified structural weakening of the cold end of the bricks in service as a result of vapourization of brick constituents into vacuum (1). It is of interest to note here that the thermal expansions of Fig. 16, although essentially linear, indicate that expansion commences only after the specimens reach a temperature several degrees above room temperature. This is attributed to the initial expansion being taken up internally within the pores and grain boundaries of the materials. In this respect, a perceptible lag in onset of measured expansion can be seen for the sample from the cold end of the used brick, indicating increased porosity.

Vapourization Loss of Oxides into Vacuum

Previously reported work had demonstrated the vapourization into vacuum of MgO and Cr_2O_3 at high temperatures (1). Similar observations have been reported by Orlov et al. and by Suvorov et al. (2,3). This work showed that vapourization, primarily of MgO, resulted in destruction of the bond between the grains at the surface and increased porosity at some depth, which would be expected to lower the strength of the bricks at the cold end and enable increased slag penetration. Some further confirmatory studies were conducted.

As the phenomenon was first detected by changes in the vapour pressure of the vacuum furnace during heating of test cups, this methodology was used, along with weight loss determinations, to document the behaviour of the

test specimens. The vapour pressure changes for 4 specimens are shown in Fig. 17 and the accompanying weight losses in Table 3.

Sample A was a small cube of rebonded fused-grain chrome-magnesia brick, scheduled for test at 1750°C, but a problem with the temperature controller resulted in a significant but indeterminate overtemperature. It is of interest for the high vapour pressure maintained over a period of 3 hours. On completion of the run, the presence of chromium sesquioxide was observed, indicating that the chrome spinel had dissociated:

$$MgCr_2O_4 \rightarrow MgO + Cr_2O_3$$

On dissociation, the MgO vapourized (resulting in increased vapour pressure) whereas the less volatile Cr_2O_3 precipitated out directly or, more probably, recrystallized from a small amount of melt present at this temperature.

Sample C represents a re-run of the above at 1750°C for 3 hours, and shows a more normal early maximum vapour pressure of 65 Pa, reducing to 35 Pa over the 3 hours. The structure of the treated specimen surfaces was as previously reported, featuring ghosts of the fused grains outlined by spinel blebs with the periclase removed preferentially by vapourization (Fig. 18). Specimens A and C demonstrate the expected temperature dependence of rate and extent of vapourization.

Sample B was a test cup left over from the cup tests, heated at 1750°C. Owing to its geometry, significantly more surface area was exposed and the thickness of the section was much reduced. This is reflected in the high initial vapour pressure, reducing to normal after about 2 hours. This condition is not representative of normal practice, but might be approached if a ladle lining were badly fractured by thermal shock.

For comparison, sample D was a cube of periclase brick, heated at 1650°C for 5 hours. The relatively high vapour pressure at this lower temperature reflects the higher MgO content. The initial high vapour pressure probably is a function of irregularities over the sawn surfaces: as these were removed by vapourization and the surfaces smoothed to an essentially constant area, the rate of vapourization decreased, becoming essentially constant, but remained at a higher level than for the chrome-magnesia at 100°C higher temperature.

Previous work (1) had shown the preferential vapourization of MgO. Figure 19 shows the morphology of a sample heated at 1650°C for 3 hours:

ghost features of fused grains are outlined by the remnantal spinel blebs within and around the grain boundaries. A fracture surface at right angles to the face is shown in Fig. 20, where the porosity between the primarily chrome spinel crystals at the surface (upper right), with resultant destruction of the intergranular bonding, can be seen to diminish with depth. Nevertheless, vapourization occurs throughout the mass, as shown in Fig. 21, a fracture surface about 5 cm behind the slag-penetrated zone of a used brick, where the evident porosity and rounding of the edges and corners of the grains clearly bespeak the loss of material by vapourization when compared with a fracture surface from an unused brick (Fig. 22).

The porosity related properties, determined according to ASTM Test Method C20-74, "Apparent Porosity, Water Absorption, Apparent Specific Gravity, and Bulk Density of Burned Refractory Brick by Boiling Water", showed the apparent porosity of the cold end of a used brick to average 15.22% vs. 12.48% for an unused brick; a water absorption of 4.68% vs. 3.75%; and a bulk density of 3252 kg/m^3 vs. 3372 kg/m^3. Obviously, heating the ladle lining to high temperature under vacuum will render the bricks more prone to deeper slag penetration during ensuing heats as well as weakening the structure and making it more susceptible to failure by thermal shock on further temperature cycling.

CONCLUSIONS

Microstructural examination by SEM and elemental distribution studies by EDXR serve well to confirm and further elucidate the mechanisms of degradation of the rebonded fused-grain chrome-magnesia bricks used to line the slagline zone of VOD/VAD ladles. The modes of failure include corrosion by the slag (and, undoubtedly, erosion of the dissolved and partially dissolved materials) and spalling.

The silica and calcia of the slag along with minor manganese oxides react aggressively with the components of the refractories, particularly the periclase phase, forming complex melts that crystallize on cooling to mixtures of forsterite, akermanite and montcellite and complex solid solutions of Ca-Mg-Mn silicates. Iron dissolved in the slag appears to diffuse throughout the periclase phase, which would be expected to render it even more susceptible to corrosion. Chrome and alumina in the slag, on the other hand, appear to recrystallize as high-temperature spinels of variable composition that are

more resistant to corrosion than the periclase. Slag attack occurs on the exposed surfaces and at depth owing to penetration of slag into the pores and, more importantly, along grain boundaries. Thus, a large area is exposed to dissolution by slag and, in addition, the presence of a liquid phase in the intergranular boundaries renders the grains susceptible to erosion by the highly agitated slag during oxygen blowing and argon bubbling, and by convection currents set up in the electric-arc heated VAD vessels. As would be expected from considerations of physical chemistry, the extent of slag attack increases with increased temperature and time.

The most resistant microstructures is that characterized by fused periclase grains rimmed by and permeated with exsolved blebs of chrome spinel, which tend to protect the less resistant magnesia phase. A less resistant structure comprises large periclase grains directly bonded to large discrete chrome spinel crystals. These are assumed to result from imperfect fusion: they tend to occur in zones or layers, possibly the result of minor segregation during filling of the moulds and pressing of the rebonded brick. Because the periclase is exposed to dissolution in the slag, these are zones of weakness with respect to slag attack. During dissolution of these materials any dissolved gases will be released, along with magnesia and chrome vapours from the liquid. When the surrounding pores are blocked with liquid slag, internal gas pressure will build up in these zones, leading to bloating of the type observed in the cup tests and the lenticular openings frequently observed in the slag-penetrated zones of the used bricks. In the latter, the voids occur at various depths and are aligned with the hot face, hence represent planes susceptible to failure under thermal shock.

Spalling attributed to thermal shock plays a role in degradation of the ladle linings, but its actual impact is difficult to assess. Observation of a ladle during removal of the lining showed evidence of spalling in some obvious disparities in length of the residual bricks. On their removal, however, many more bricks were seen to be cracked behind the hot face, although the spalls had remained in place and continued to perform at least part of their function. It appears that most of the spalls do not fall off until they have been considerably thinned by the processes of corrosion and erosion. Most of the cracks were filled with slag and corrosion products or, frequently, with metal that, owing to its greater density, had probably replaced slag.

Most of the cracks were of the primary type, i.e., roughly parallel to the hot face, with little evidence of secondary cracking, at right angles to the hot face. However, the orientations and distortions of the fracture planes suggested that they had originally followed a surface of slag penetration in the same manner as the failure in the laboratory thermal shock tests, although the slag had penetrated beyond the crack in subsequent heats. Given that the coefficient of thermal expansion is little altered by slag penetration, it seems likely that failure along this plane is related to structural weakening of the unpenetrated brick immediately behind the plane of penetration owing to vapourization of constituent oxides.

Selection of refractories is always a compromise between refractoriness, corrosion resistance, thermal shock resistance and cost. The rebonded fused-grain chrome-magnesia bricks in use are currently deemed the most cost beneficial material for this service. Some improvement in quality would appear possible, particularly to ensure that the fused grain comprised only the type with exsolved chrome spinel. Denser bricks, e.g., the same materials in fusion-cast form, would unquestionably be more resistant to slag attack and to vapourization of constituents, which would be restricted to the surfaces only: however, the high cost and greater susceptibility to thermal shock renders their application of questionable value. Dense zirconia and alumina appear to suffer from the same considerations. Nevertheless, it might be useful to examine these and other possible alternatives using the methodologies employed in these studies to explore their potentials. Some changes in furnace practice might be useful, e.g., use of more-basic slags if such are compatible with the necessary steel-making requirements. The company has reported on some inconclusive trials substituting dolomite for limestone in the slag composition. In theory, this should increase the MgO saturation of the slag and inhibit dissolution of MgO from the brick, which is the major source of attack. Further tests to establish the required level of MgO in the slag may be useful.

ACKNOWLEDGEMENTS

The writers wish to express their gratitude to the Atlas Steels Company, Welland, Ontario for supplying the samples necessary for this study. Thanks are also due to the staff of the Mineral Sciences Laboratories, CANMET who contributed to this project, particularly Mr. G. Lemieux, who assisted with all the laboratory tests, Mssrs. J.M. Beaulne and J.J.Y. Bourgoin, who prepared the polished and thin sections, and Dr. D.C. Harris and Mr. D.R. Owens for the electron-optical work.

REFERENCES

1. Quon, D.H.H. and Bell, K.E. "Degradation of slagline chrome-magnesia bricks in secondary steelmaking under vacuum environment: a progress report"; Division Report MRP/MSL 80-83 (IR); CANMET, Energy, Mines and Resources Canada; 1981.

2. Orlov, V.A., Sokolov, A.N., Polonskii, Yu.A., Caponov, Ya.G., Mezentsev, E.P., Simonov, K.V., Kabonov, V.S., Suvoror, S.A., Kuznetsov, G.I., Chermak, A., and Gavlik, V. "New refractories for plant handling the vacuum treatment of steel outside the furnace"; Refractories 21:67-80; 1980.

3. Suvorov, S.A., Mel'nikov, A.D., Orlov, V.A., Simonov, K.V., Bocharov, L.D., Kuznetsor, G.I., Pereplitsyn, V.A., and Pivnik, L.Ya. "Wear of magnesia spinel refractories in production vacuum-processing steel plant"; Refractories (Translated from Russian OGNEUPORY) 21:145-153; 1980.

Table 1. Compositions of the slags used for laboratory cup tests

Sample no. *	Oxides, mass %						
	SiO_2	Cr_2O_3	Al_2O_3	CaO	MgO	Fe_2O_3	$CaO:SiO_2$
1.	33.3	0.63	10.5	44.8	8.81	0.97	1.34
2.	38.7	3.98	6.47	41.85	7.10	1.90	1.08
3.	38.97	0.67	10.32	35.88	12.69	0.98	0.92
4.	38.15	0.43	10.04	36.59	12.79	0.94	1.04
5.	33.61	0.49	7.60	39.42	17.85	1.07	0.85
6.	37.9	0.80	8.53	39.93	11.80	1.04	0.95

*1. Ladle after teeming, heat J5998T409A1
2. Ladle after VOD, heat J5998T4509A1
3. Ladle after teeming, heat J6001T304A2
4. Ladle after VOD, heat J6001T304A2
5. Ladle after teeming, heat J6002T431A2
6. Ladle after VOD, heat J6002T431A2

Table 2. Luminescent phases in the slag component and their approximate compositions

Luminescent colour	Morphology	Chemical composition
Green	Octohedron	Mg, Al oxides with trace of Mn, Ca, Ti
White	Prismatic	Ca-Mg-Mn silicate
Bluish	Prismatic	Ca silicate with traces of Mg, Ti
Reddish	Prismatic	Ca-Mg-Al silicate with trace of Mn
Orange	Prismatic	Ca-Mn silicate with trace of Mg

Table 3. Test conditions for vapourization studies

Sample	Weight g	Temperature °C	Time h	Weight Loss mass %
A	4.9833	1750 *	5	- **
B	94.4623	1650	4	3.15
C	5.4866	1750	3	17.30
D	114.0493	1650	2	2.00

* Error in temperature reading:

** Overtemperature caused partial melting

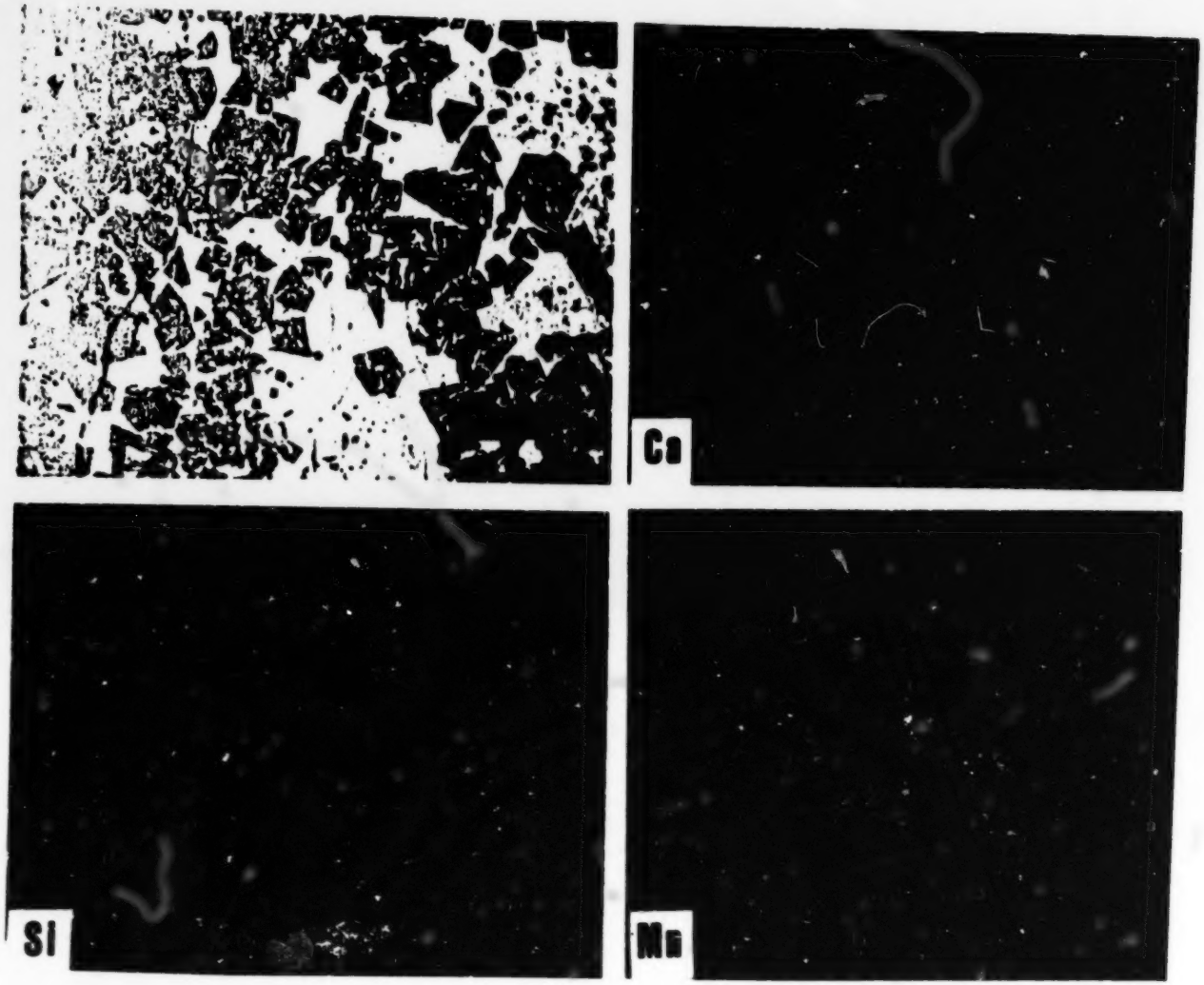

Fig.1 - SEM micrograph of typical slag-penetrated zone of a used brick, with EDXR maps of the major slag components Ca, Si and Mn

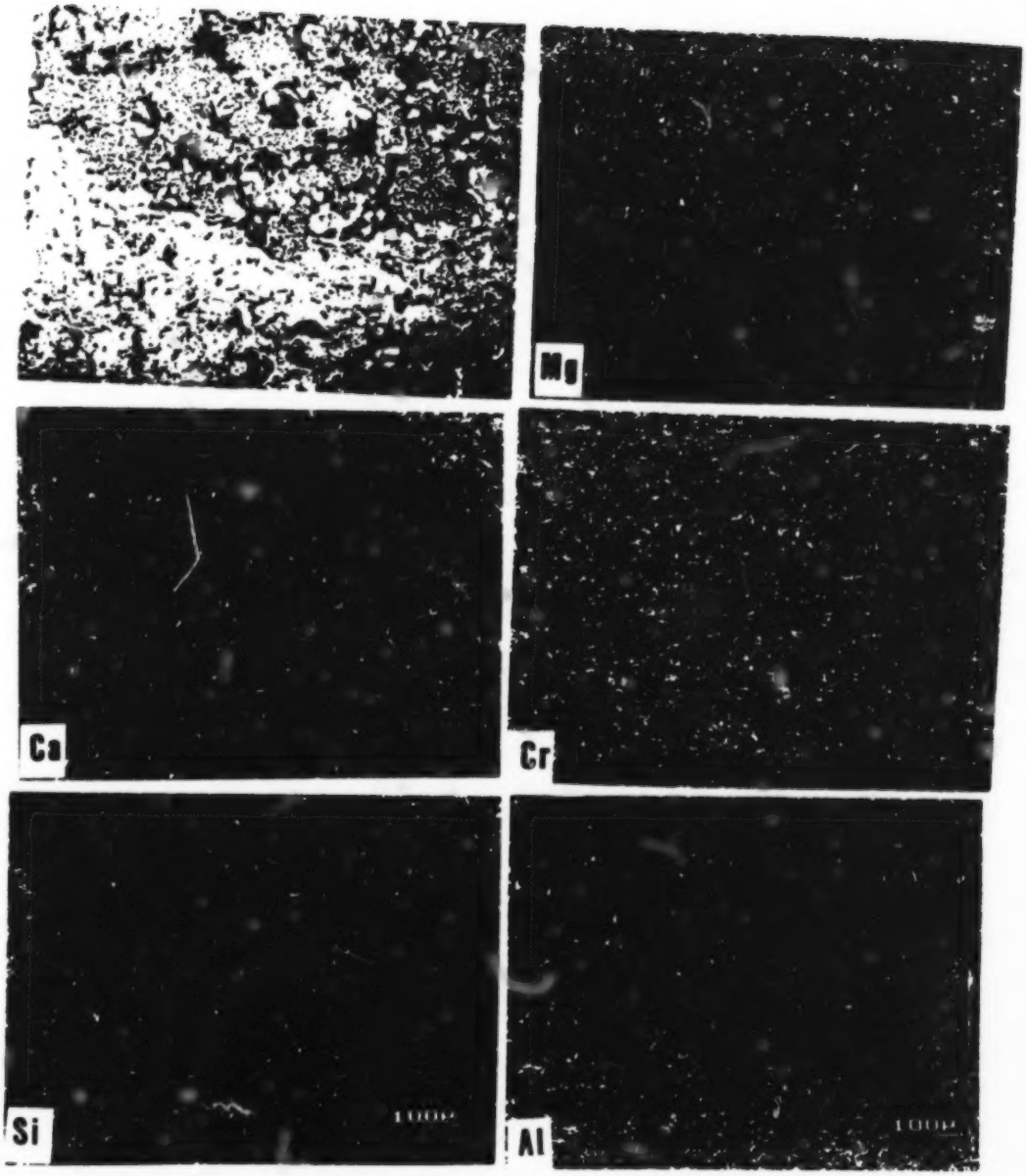

Fig. 2 - SEM micrograph of a fresh slag/brick contact zone, with EDXR maps showing the distribution of elements of interest

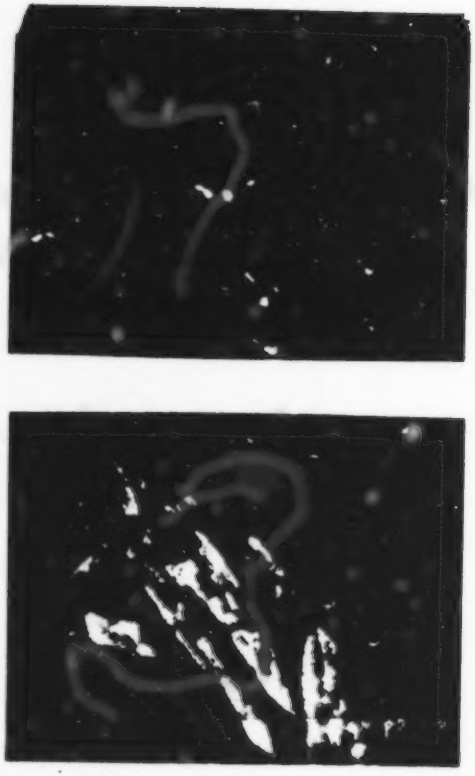

Fig. 3 - SEM micrographs of luminescent phases in slagged brick;
Top: green octahedra with orange reaction rims,
Bottom: white acicular crystals

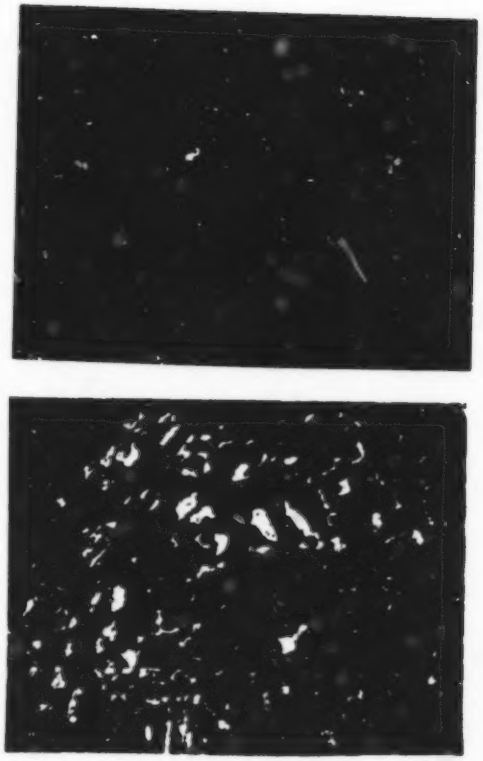

Fig. 4 - SEM micrographs of luminescent phases in slagged brick;
Top: green octahedron with reddish core,
Bottom: green octahedron with orange rim in a field of blue dendrites

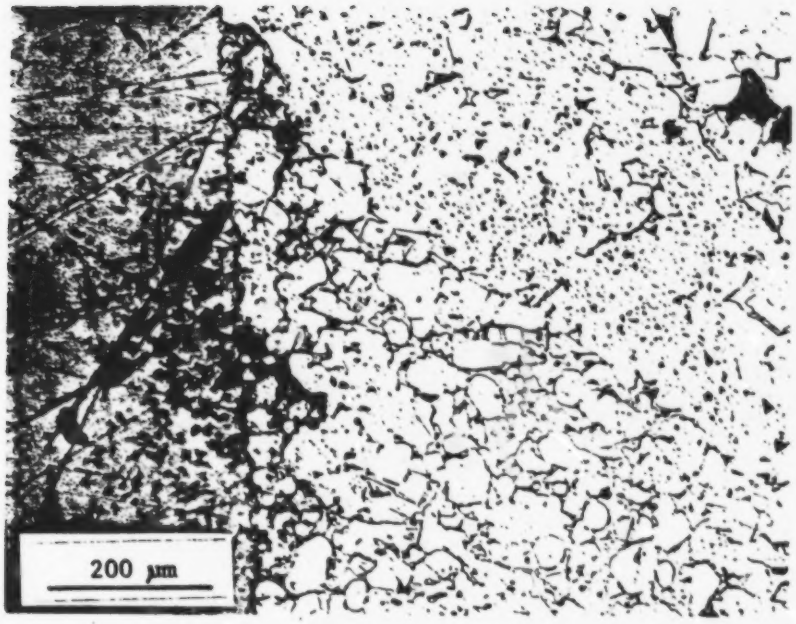

Fig. 5 - Optical micrograph showing slag penetration into wall of cup, x 125

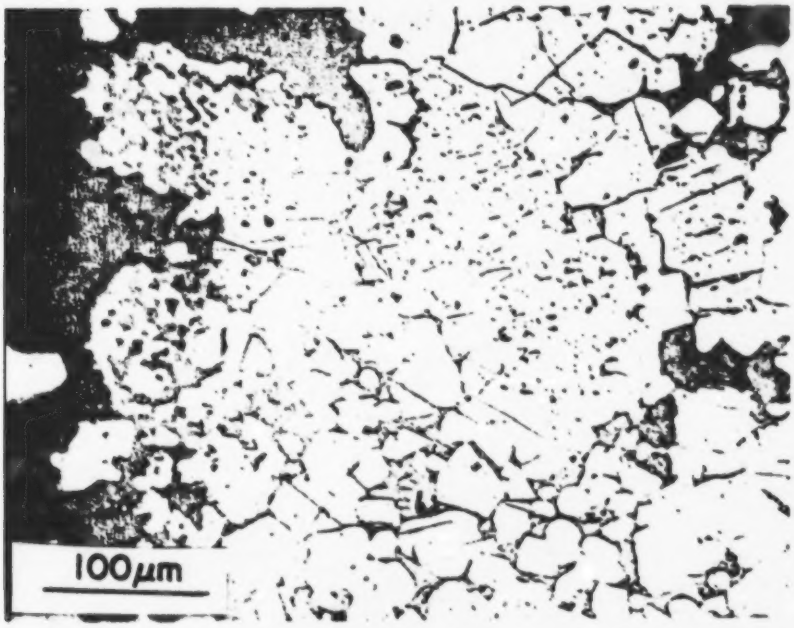

Fig. 6 - Optical micrograph showing slag penetration into cup wall, x 250

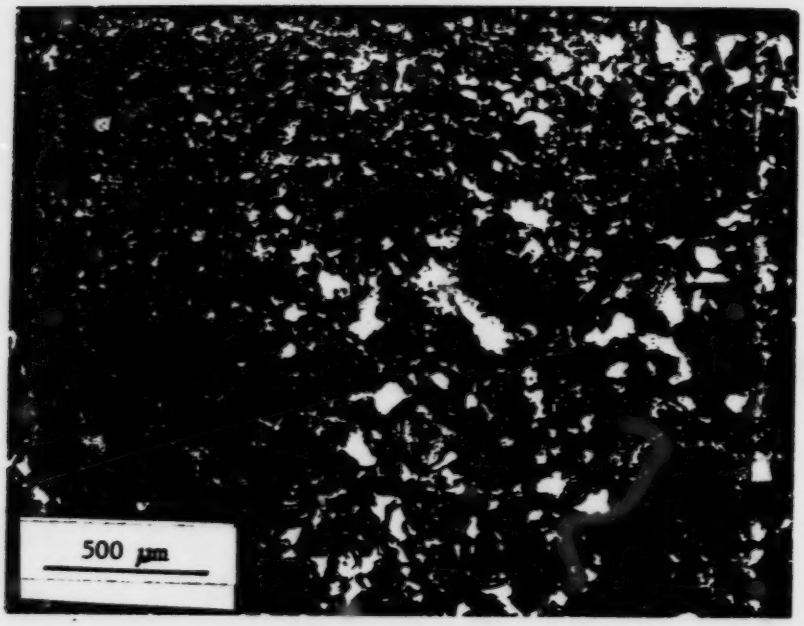

Fig. 7 - Thin section of slag-penetrated cup showing silicates (white) in pores and along grain boundaries; transmitted light, crossed polars, x 250.

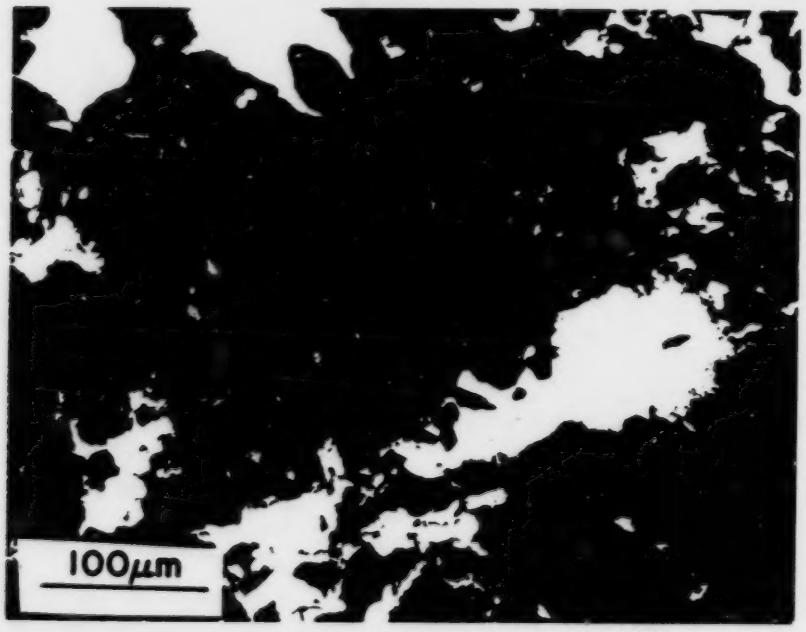

Fig. 8 - Enlarged section of Fig. 7 showing silicate crystal habit; acicular and dendritic growths, x 250.

Fig. 9 - Polished section of slag-penetrated cup, x 125.

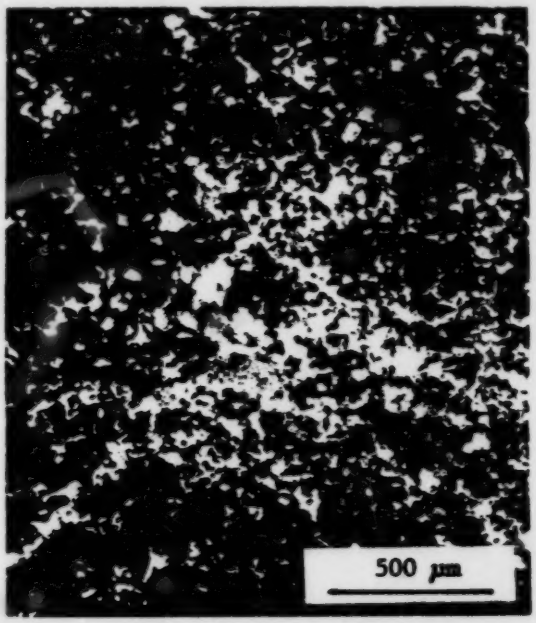

Fig. 10 - Thin section of slag-penetrated cup, transmitted light, crossed polars, x 50.

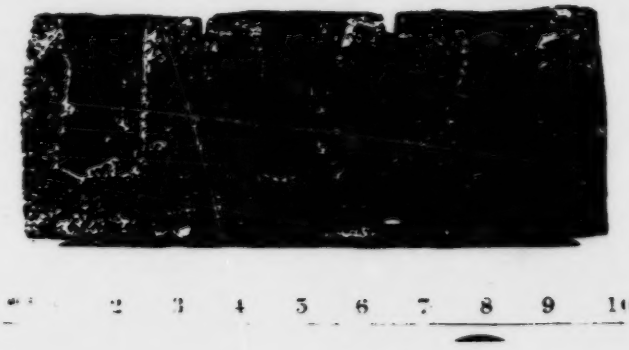

Fig. 11 - Cross-sectioned cups after two cycles at 1700°C for 3 hours.

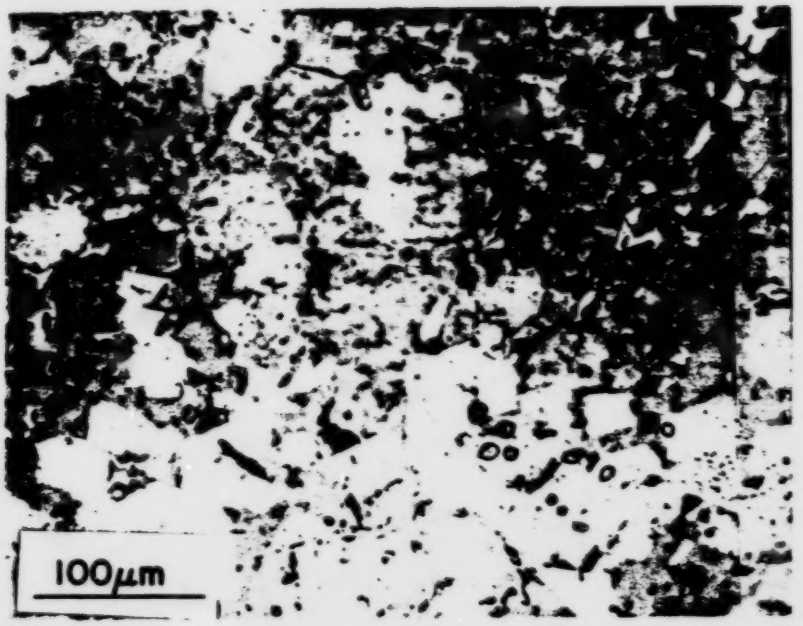

Fig. 12 - Optical micrograph of fully slagged cup, showing similarity to microstructure of used brick, x 250. (light phase: wustite?)

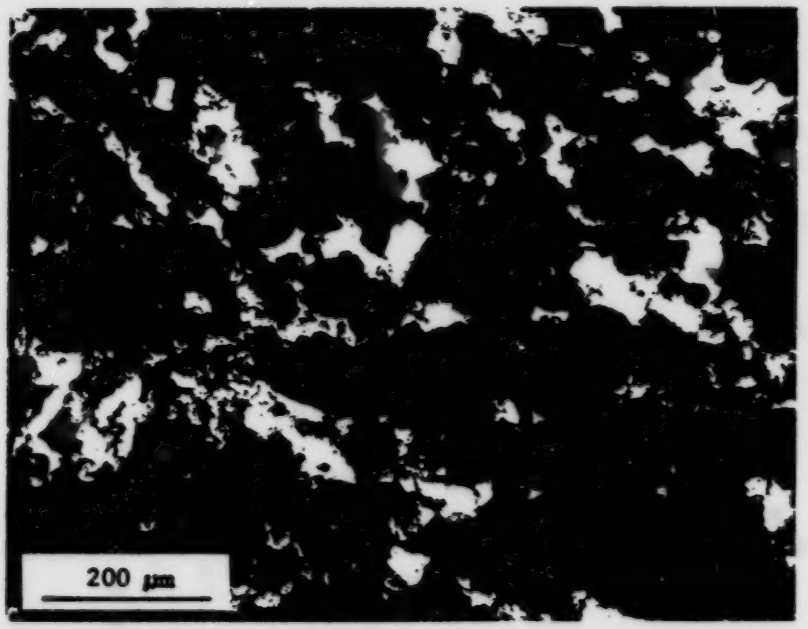

Fig. 13 - Thin section of fully slagged cup, showing interstitial silicates (white), transmitted light, crossed polars, x 125.

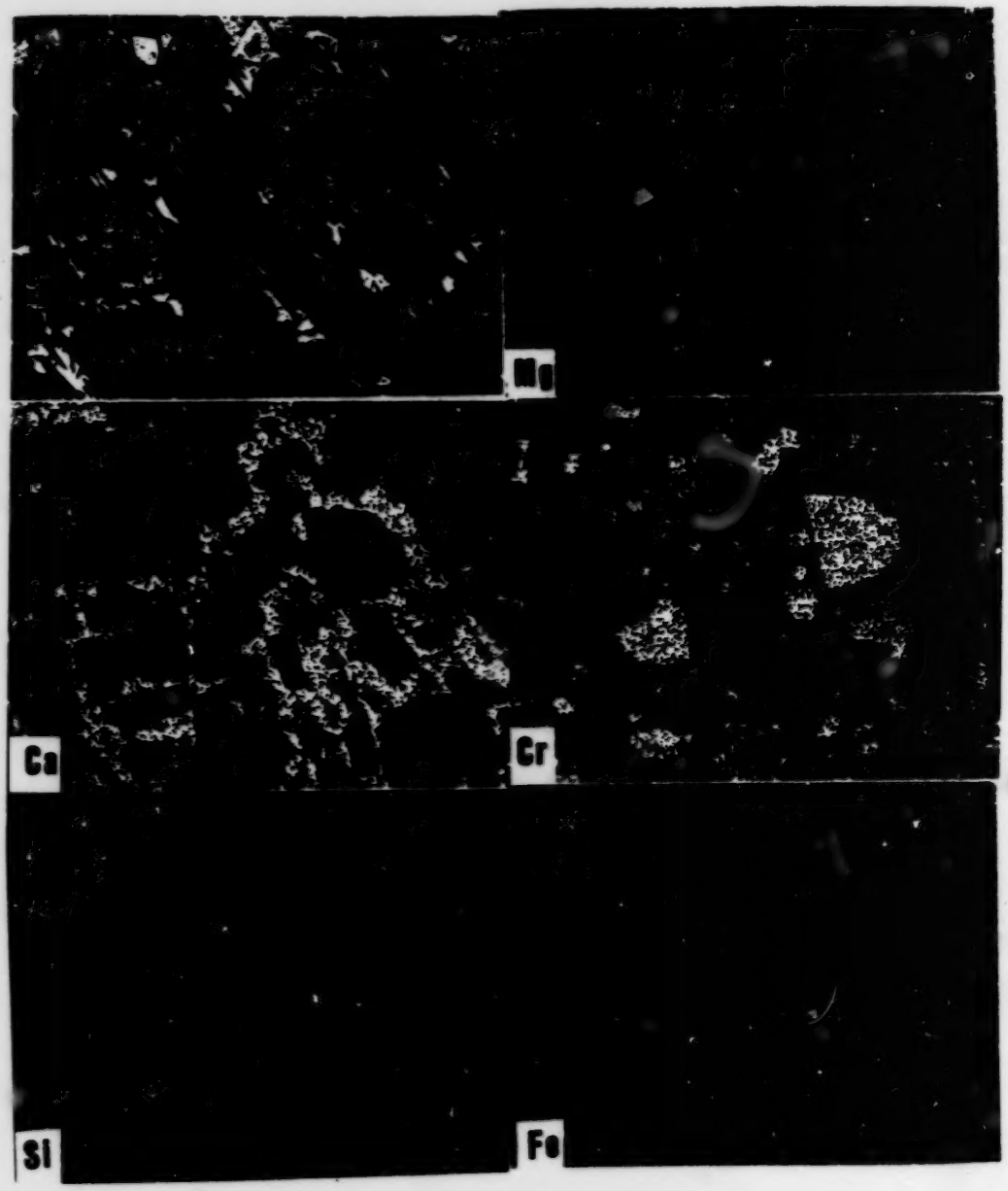

Fig. 14 - SEM micrograph of fully slagged cup, with EDXR maps of distribution of elements of interest.

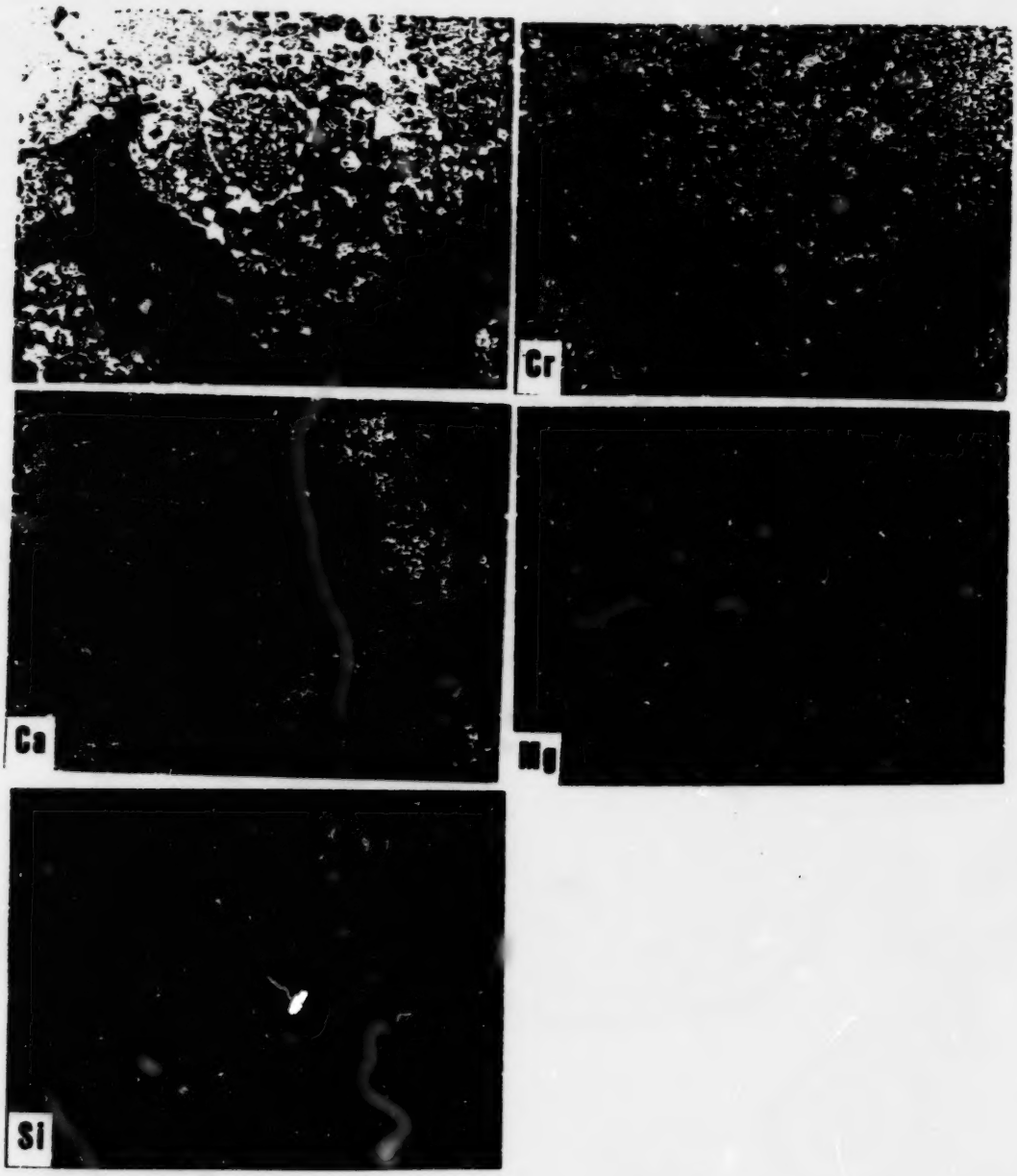

Fig. 15 - SEM micrograph of fully slagged and bloated cup, with EDXR maps of elemental distribution of principal slag components.

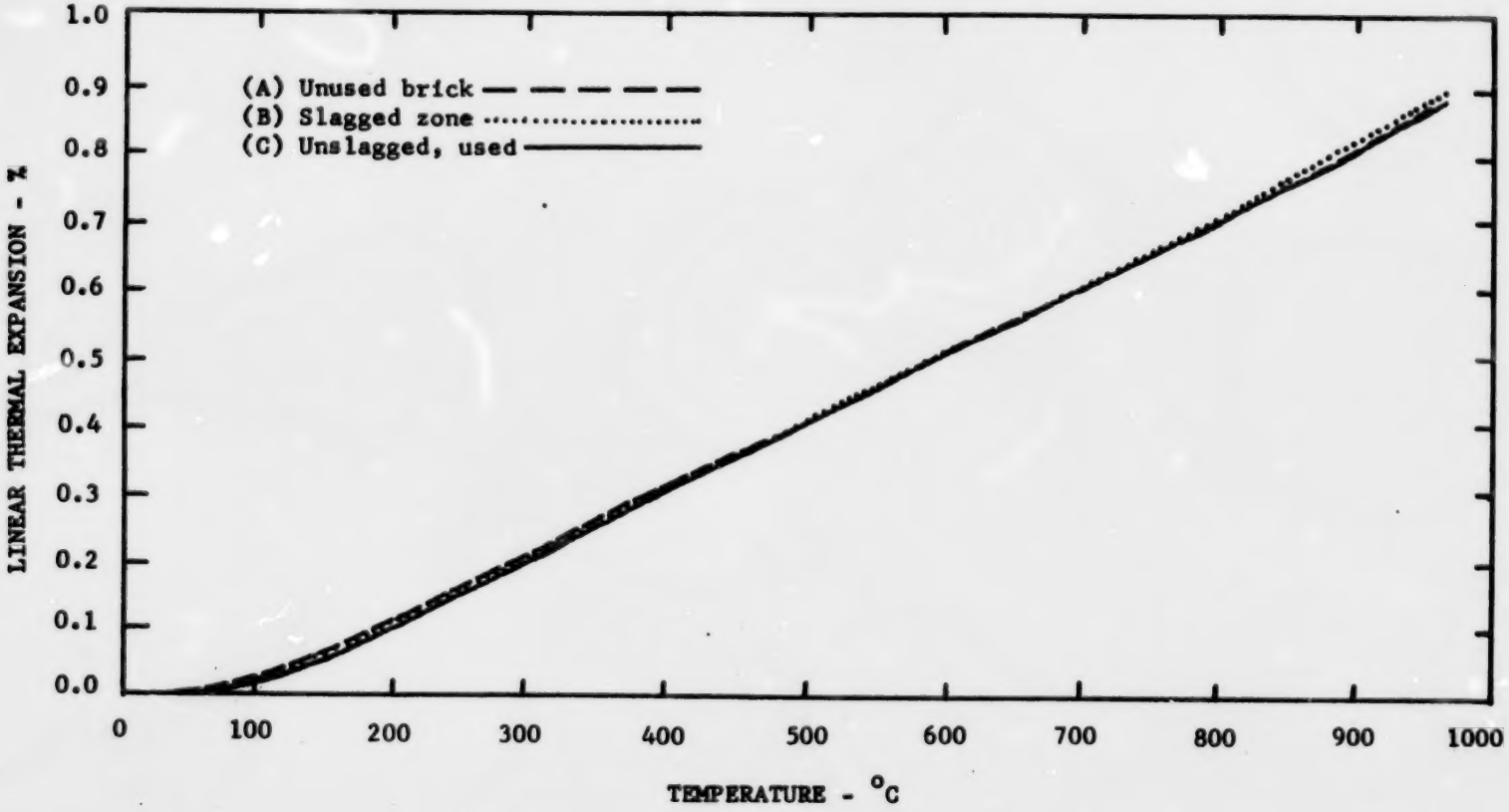

Fig. 16 - Linear thermal expansion of (A) unused brick, (B) slag penetrated zone of used brick, and (C) unslagged (cold) end of used brick.

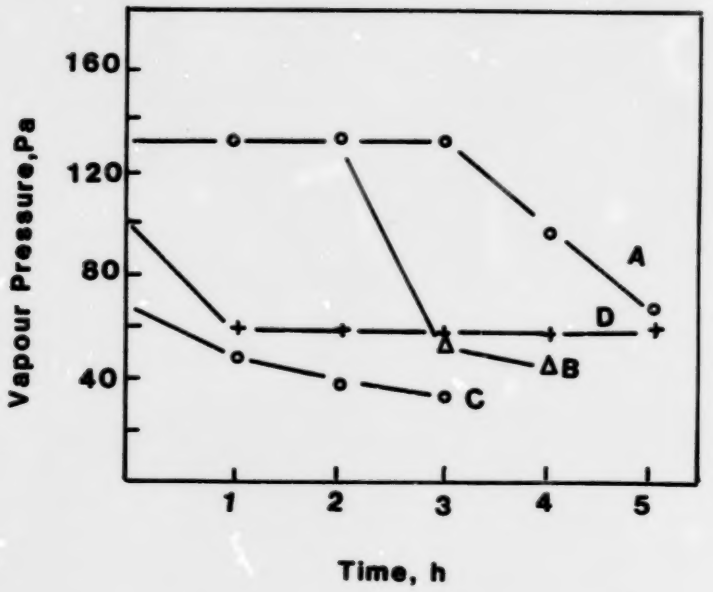

Fig. 17 - Furnace vapour pressure profiles during oxide vapourization: (A) rfg Cr-Mg brick, overtemperature, (B) rfg Cr-Mg test cup, 1750°C, (C) rfg Cr-Mg brick, 1750°C, (D) periclase brick, 1650°C.

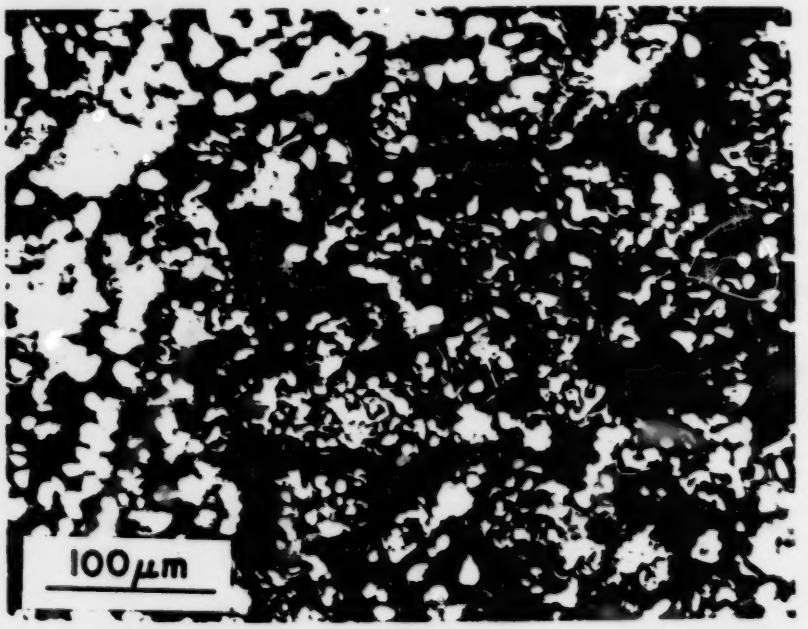

Fig. 18 - Optical micrograph of vapourized surface (1750°C for 3 hours) x 250.

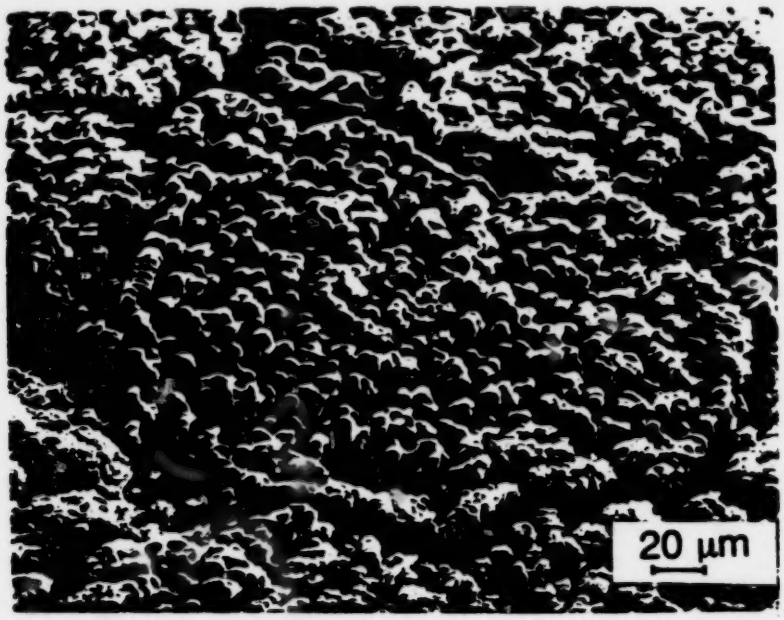

Fig. 19 - SEM micrograph showing exsolved spinel phase outlining the ghost grains of periclase (1650°C for 3 hours).

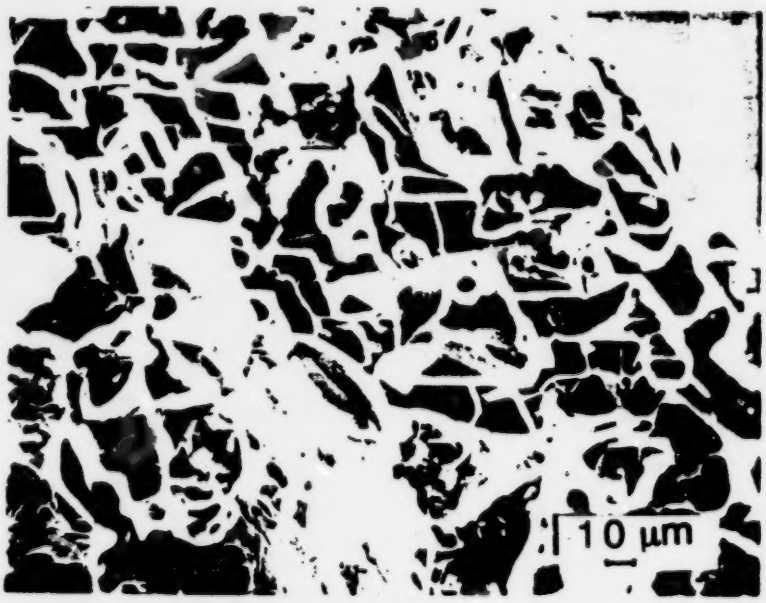

Fig. 20 - SEM micrograph of fracture surface perpendicular to Fig. 19.

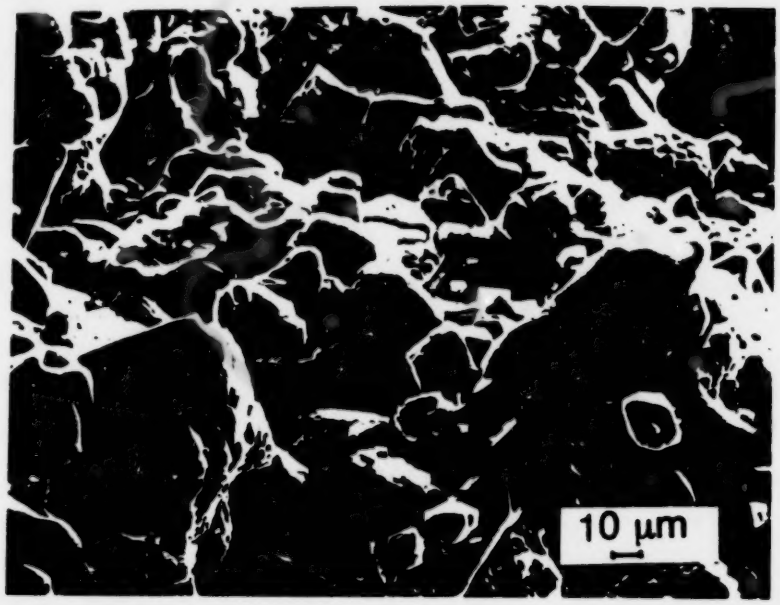

Fig. 21 - Fracture surface of unslagged (cold) end of used rfg Cr-Mg brick.

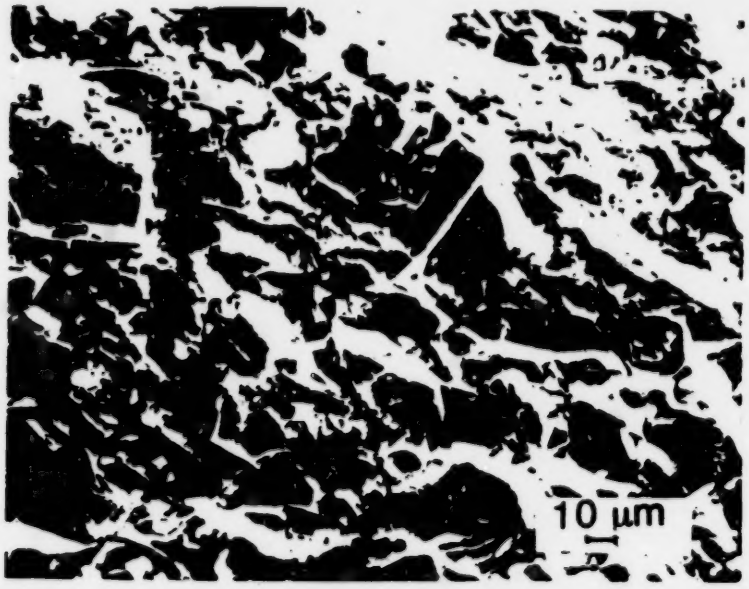

Fig. 22 - Fracture surface of unused rfg Cr-Mg brick.